Workflow for Managing Impurities in an Integrated Crystallization Process

Yuen S. Cheng, Ka W. Lam, and Ka M. Ng
Dept. of Chemical and Biomolecular Engineering, The Hong Kong University of Science and Technology, Clear Water Bay, Kowloon, Hong Kong Special Administrative Region

Christianto Wibowo
ClearWaterBay Technology, Inc., Pomona, CA 91789

DOI 10.1002/aic.12027
Published online September 28, 2009 in Wiley InterScience (www.interscience.wiley.com).

A workflow consisting of experiments, modeling, and synthesis is presented for managing the impurity content in the product crystals of a crystallization process taking into consideration the entire train of crystallization and downstream processing steps. Experiments on solid–liquid equilibrium, impurity inclusion, washing, and deliquoring are designed in such a way that the experimental data or the model parameters derived from these data can be readily used for process design. Guidelines for experimental design and tradeoffs in process synthesis are discussed. The workflow is illustrated using the purification of Vitamin C (ascorbic acid) as a case study. © 2009 American Institute of Chemical Engineers *AIChE J,* 56: 633–649, 2010
Keywords: process development, impurity management, crystallization, downstream processing, solid–liquid separation

Introduction

Controlling the impurity content in the final product crystals of a crystallization process is a crucial issue because of its significant economic impact. Commodity and specialty chemicals are often sold in various grades with substantially different prices based on the purity level, whereas active pharmaceutical ingredients can be worthless if they do not meet certain purity specifications.

The undesired impurities can be incorporated into the crystals during growth, trapped inside agglomerates of crystals, adsorbed on crystal surfaces, or incompletely removed during filtration, washing, and deliquoring of the crystals downstream of the crystallizer(s). Much has been done to elucidate the relevant phenomena. For example, the amount of inclusion impurity inside the crystal is closely tied to particle size, growth rate, and agglomeration rate, which in turn are affected by operating variables, such as crystallization temperature, cooling rate, stirring rate, and presence of surfactant.[1–5] The degree of impurity removal is dependent on the wash ratio in washing and the pressure difference in deliquoring.[6,7] At present, it is still not possible to predict, from first principles, these behaviors quantitatively, and experimental testing is essential in practice.

In contrast, only limited effort has been made on the design of processes to meet the impurity target from a systems perspective. A hierarchical approach is available for synthesizing the necessary flow sheet and specifying the destinations of the reaction solvent, mother liquor, wash liquid, recrystallization solvent, and drowning out solvent systematically.[8] A subsequent study clarifies the possible influence of crystal size distribution on the downstream units, and the ways in which the desirable crystal size distribution that offers minimum adverse impacts can be realized in the crystallizer(s).[9] In these design procedures, the information on all model parameters as well as the relevant experimental data is assumed to be given. This approach is similar to most of the process design literature in which experiments

Correspondence concerning this article should be addressed to K. M. Ng at kekmng@ust.hk

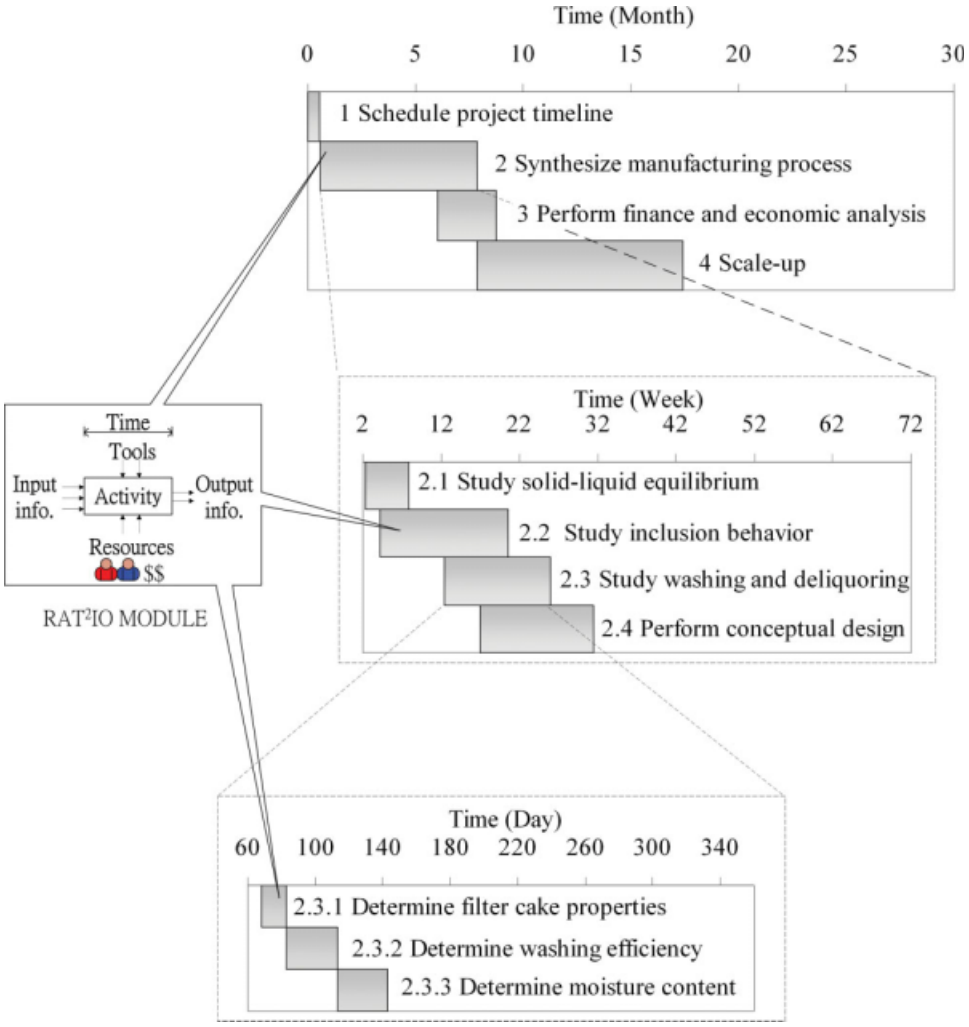

Figure 1. The objective-time chart for impurity management.

[Color figure can be viewed in the online issue, which is available at www.interscience.wiley.com.]

are seldom considered and, thus, it only captures part of how most industrial processes are actually developed.

For new processes, only limited physical and chemical information is known at the early stage of process design. Concurrent experimental data acquisition and process synthesis are the key for designing a better process and for shortening time-to-market.[10] By identifying the dominant physical and chemical phenomena, modeling serves as an intermediary between experiments and process design.

The objective of this article is to formulate a workflow that combines experiments, modeling, and synthesis to come up with an integrated crystallization process involving the entire train of crystallization and downstream processing steps to meet the final product purity target. Emphasis is placed on the methodologies for collecting experimental data, using models in data analysis, and synthesizing a process based on these results. Using ascorbic acid as a case study, it demonstrates how these activities are integrated in process development. Guidelines and best practices derived from our industrial experience are highlighted throughout the article. Scheduling of the R&D activities is considered alongside the workflow.

Workflow for Impurity Management

The workflow begins with an objective-time chart as shown in Figure 1.[11] Objective 1 is part of project management which specifies the tasks to be completed in a given time horizon. Each objective can be broken down into subobjectives. Such a hierarchical view of the development project informs every project team member what are being done to achieve the overall goal. Also, it highlights the tasks that can be carried out concurrently, thereby reducing the overall development time. However, it is often difficult to identify in advance all the necessary experiments particularly when unanticipated results are obtained. Thus, some experiments need to be repeated and hence new experiments are scheduled. Objective 2 is to synthesize a manufacturing process to meet final product purity specifications. It can be decomposed into subobjectives: studies of solid–liquid equilibrium (SLE), impurity inclusion, washing, and deliquoring performance and conceptual design. These subobjectives can be broken down further. For example, the washing and deliquoring performance study includes the determination of filter cake properties, dependence of washing efficiency on wash ratio, residual moisture content as a function of pressure or vacuum level, among others.

Table 1. Subobjectives for Synthesizing Crystallization Downstream Process to Achieve Desired Impurity Levels

Objectives	Input Information	Activities	Tools	Resources	Time (month)	Output Information
2.1. Study solid-liquid equilibrium (SLE) behavior	• Physical and chemical properties of the product • Solvent under consideration • Existing impurities • Product specifications	• Determine SLE phase diagram • Define crystallization conditions using phase diagram	• Experimental setup for SLE data acquisition • Computation tools for data regression	• A chemical engineer with experience in SLE data acquisition and analysis • Budget for personnel or outsourcing this task	1.5	• SLE data • Possible crystallizer feed compositions
2.2. Study inclusion behavior	• SLE data • Crystallizer feed compositions and conditions	• Develop analytical methods for impurity concentration • Carry out crystallization tests for different operating parameters	• Crystallization setup • Analytical technique	• A chemical engineer with experience in crystallization and analytical methods	4	• Analytical methods for impurity concentration • Dependence of inclusion level on experimental parameters.
2.3. Study washing and liquoring performances	• Crystallizer effluent compositions • PSD information	• Carry out filtration, washing and deliquoring experiments	• Modeling • Setup for filtration–washing–deliquoring experiments	• A chemical engineer with experience in filtration–washing–deliquoring	3.5	• Empirical correlation between impurity level and wash ratio • Dependence of final cake wetness on deliquoring time and pressure difference
2.4. Perform conceptual design	• Inclusion data • Washing and deliquoring performance • Process synthesis procedure	• Generate possible scenarios • Design process flowsheets • Target equipment specifications	• Simulation tools • Equipment models	• A chemical engineer with knowledge of crystallization downstream processes synthesis	1	• Process flowsheets for different scenarios • Equipment specifications

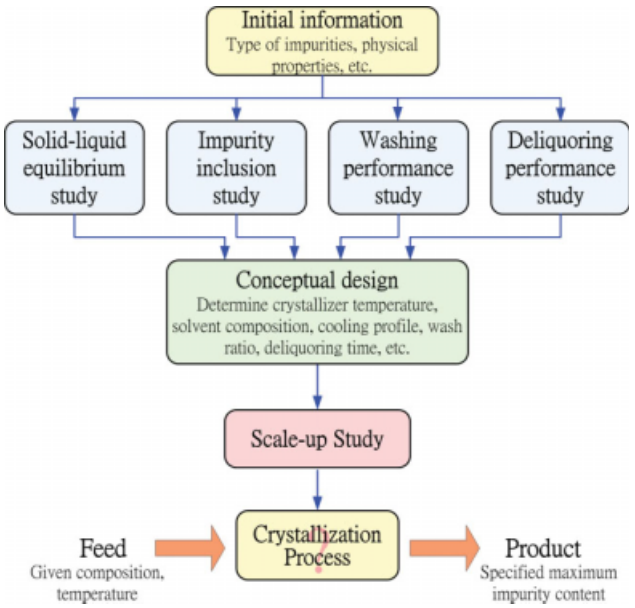

Figure 2. The tasks for impurity management.

[Color figure can be viewed in the online issue, which is available at www.interscience.wiley.com.]

To achieve the objectives and subobjectives, RAT^{2}IO modules are used (Figure 1). The acronym stands for *r*esources, *a*ctivities, *t*ime, *t*ools, input/output *i*nformation, and *o*bjective. We identify in advance the resources (money and people) required to complete certain activities (experiments, modeling, and synthesis) within a specified period of time using proper tools (experimental setup or software) to generate the necessary information so as to meet the given objective. For instance, the RAT^{2}IO modules listed in Table 1 is used to achieve the process synthesis objective.

These studies constitute the major components of the workflow for impurity management (Figure 2). Solid–liquid equilibrium study is needed to confirm the phase behavior of the system consisting of the desired product and major byproducts. Thus, these impurities are thermodynamically based and can be avoided by performing crystallization well within the crystallization region of the product. However, inclusion impurities can still contaminate the product crystals. These are non-crystallizing impurities that got incorporated into the solid phase during crystallization, and cannot be removed from the solid phase without dissolving the crystals. For practical purposes, impurities adsorbed on the surface of the crystals are included in this type if they are not removable during washing. Impurity inclusion study is to determine the relationship between the amount of inclusion impurities and operating parameters such as crystallization yield and cooling rate, solvent composition, and so on. The washing performance study deals with surface impurities that refer to those dissolved in the residual liquid trapped inside the interstitial pores among the crystals. Finally, the effect of deliquoring time and pressure difference on the cake wetness is quantified in the deliquoring performance study. With input information such as the type and amount of impurities in the feed stream, physical properties of the pure components, and mixtures involved, and so on, experimental data from these studies provide the necessary information for conceptual design, during which the operating conditions of the crystallizer as well as the downstream units are specified. These conditions are then validated in a series of scale-up studies which eventually lead to an integrated crystallization process yielding a final product with the desired purity.

Case study—Ascorbic acid process

To illustrate the workflow for solving a typical industrial problem, an example on the production of ascorbic acid, better known as vitamin C, is presented. Ascorbic acid (AsA) can be produced by fermentation of D-glucose.[12] The conversion of D-glucose is close to 100%, and the reactor effluent contains mainly the product (AsA), solvent (50/50 wt % ethanol/water), and byproducts, which are the source of impurities in the product. AsA is recovered from this reactor effluent by cooling crystallization. Table 2 summarizes the available input information. Among the numerous impurities, only two of the most abundant ones, oxalic acid (OxA) and 2-furaldehyde (2-Fur), will be considered to minimize the complexity. The product specifications call for a maximum oxalic acid and 2-furaldehyde concentrations of 1000 ppm and 50 ppm, respectively.

Solid–Liquid Equilibrium Study

The solubility data for the crystallization system (solute/major impurities/solvent), if not available in the literature, have to determined experimentally. Systematic procedures such as the isothermal and polythermal methods have been developed.[13] With proper training, as little as 1 mg of solute could be used for solubility determination. Method for high-pressure systems is also available.[14,15] Time could be saved by using high throughput apparatus that performs multiple solubility measurements concurrently.[16,17] Representation of SLE data on phase diagrams for various systems, such as simple eutectic, polymorphic,[18] chiral,[19] solid solution,[20] and high-dimensional systems[21] has been developed. The crystallization temperatures and compositions at which cocrystallization of the product and impurities does not occur can be readily identified on the phase diagram.

Case study—Ascorbic acid process

The crystallization system in this case study involves the product (ascorbic acid), the impurities (oxalic acid and

Table 2. Input Information of the Ascorbic Acid Process

Product specifications	
Production rate (based on dry ascorbic acid)	40 kg h^{-1}
Maximum impurity level of oxalic acid	1000 ppm
Maximum impurity level of 2-furaldehyde	50 ppm
Reaction system	
Temperature	48°C
Reactor effluent composition	
Ascorbic acid (product)	27 wt %
Solvent (50 wt % ethanol in water)	65 wt %
By-products and impurities (oxalic acid and 2-furaldehyde)	8 wt %
Crystallization system	
Type of crystallization	Cooling
Temperature	28°C
Solids density	1650 kg m^{-3}
Filtrate density	1000 kg m^{-3}

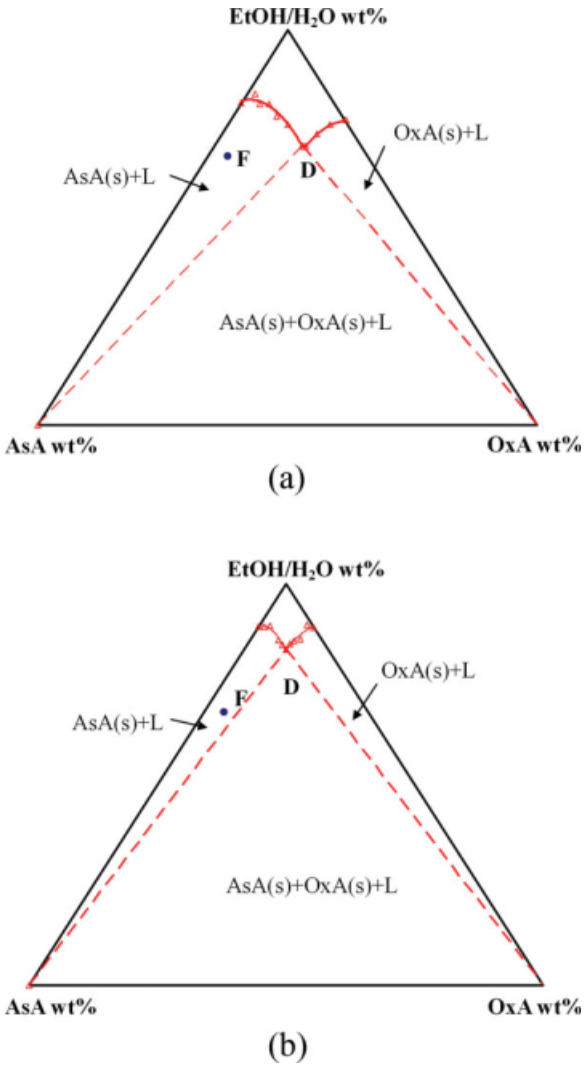

Figure 3. The isothermal phase diagrams of ascorbic acid – oxalic acid – ethanol/water system at (a) 28°C and (b) 8°C.

[Color figure can be viewed in the online issue, which is available at www.interscience.wiley.com.]

2-furaldehyde), and the solvent. As 2-furaldehyde is a liquid within the intended range of crystallization temperatures, only the ternary phase diagram of ascorbic acid/oxalic acid/solvent was determined. The experimental setup and procedure have been discussed elsewhere.[13]

The isothermal phase diagrams at 28°C and 8°C are shown in Figures 3a, b, respectively. Each data point was obtained by slowly adding the solvent to a mixture of ascorbic acid and oxalic acid of a given ratio until all solids get dissolved, while keeping a constant temperature. Two branches can be identified on the diagram: the left branch is the ascorbic acid saturation curve, whereas the right branch corresponds to oxalic acid saturation. They intersect at the double saturation Point D, which represents a solution that is saturated with both ascorbic acid and oxalic acid at this temperature. The two dotted lines extending from Point D to the AsA and OxA vertices define three crystallization regions. As the feed to the crystallizer (Point F) is located well inside the AsA(s) + L region at both temperatures, it is expected that pure ascorbic acid will be obtained on crystallization to a final temperature anywhere between 8°C and 28°C, and the coprecipitation of oxalic acid is not a concern.

Impurity Inclusion Study

The inclusion level depends on solvent composition, crystal size, and crystal growth rate which in turn is affected by the cooling rate, solvent evaporation rate, antisolvent feed rate, and so on. Crystallization experiments should be performed to identify suitable conditions to keep the impurities within acceptable limits. The most common method is to recover the crystals by filtration from the slurry after crystallization experiments and then analyze their compositions by suitable analytical instruments. In carrying out the filtration step, extra care should be taken in transferring hot and saturated slurry to a cool filter. Additional solidification may take place due to a sudden temperature drop, leading to higher yield and impurity content. In contrast, the solids in the slurry may dissolve when it is transferred from a cold crystallizer to a warmer filter. Therefore, temperature control is essential not only during crystallization, but also in the solids recovery and washing steps.

Figure 4 shows four basic designs of bench-scale experimental setups developed in our laboratory for cooling crystallization and solids recovery. They have different sizes and features. For all four setups, crystallization temperature is controlled using external oil circulating baths. The setup in Figure 4a is suitable for small volume (5–30 ml) cooling crystallization and slurry with low viscosity. The mother liquor can be completely and quickly removed by vacuum suction right after crystallization and the solids are recovered on the filter head for subsequent composition analysis. However, the small area of the filter head limits the amount of solids to be recovered and thus it is suitable for a slurry sample with a low solid/liquid ratio. The setup in Figure 4b is used for a slurry volume of 50–250 ml. The slurry can be either poured by hand or transferred through a heat insulated tubing under vacuum to the filter. The design in Figure 4c combines a crystallizer with a filter by fixing a filter disk at the bottom of the crystallizer. Crystallization takes place above the filter disk and the crystallization mixture does not fall below the filter disk when the stopcock is closed. Crystals can be collected on the filter by simply opening the stopcock and turning on the vacuum. Filtration–washing–deliquoring experiments can then be performed without a slurry transfer step. Thus, unwanted crystallization and changes in mother liquor composition due to temperature change in slurry handling is avoided. When high-pressure filtration is required, a stainless steel chamber/filter disk (Figure 4d) is used instead. Preheated pressurized air stream provides the pressure difference for filtration. The filtration temperature can be controlled by wrapping the stainless steel chamber with heating tape.

After filtration, thorough washing of the crystals to remove the residual moisture has to be performed before drying and composition analysis. Selection criteria for the wash liquid are listed in Table 3. The key requirement is that the wash liquid should not dissolve the product crystals. If such a solvent is unavailable, a solvent saturated with the

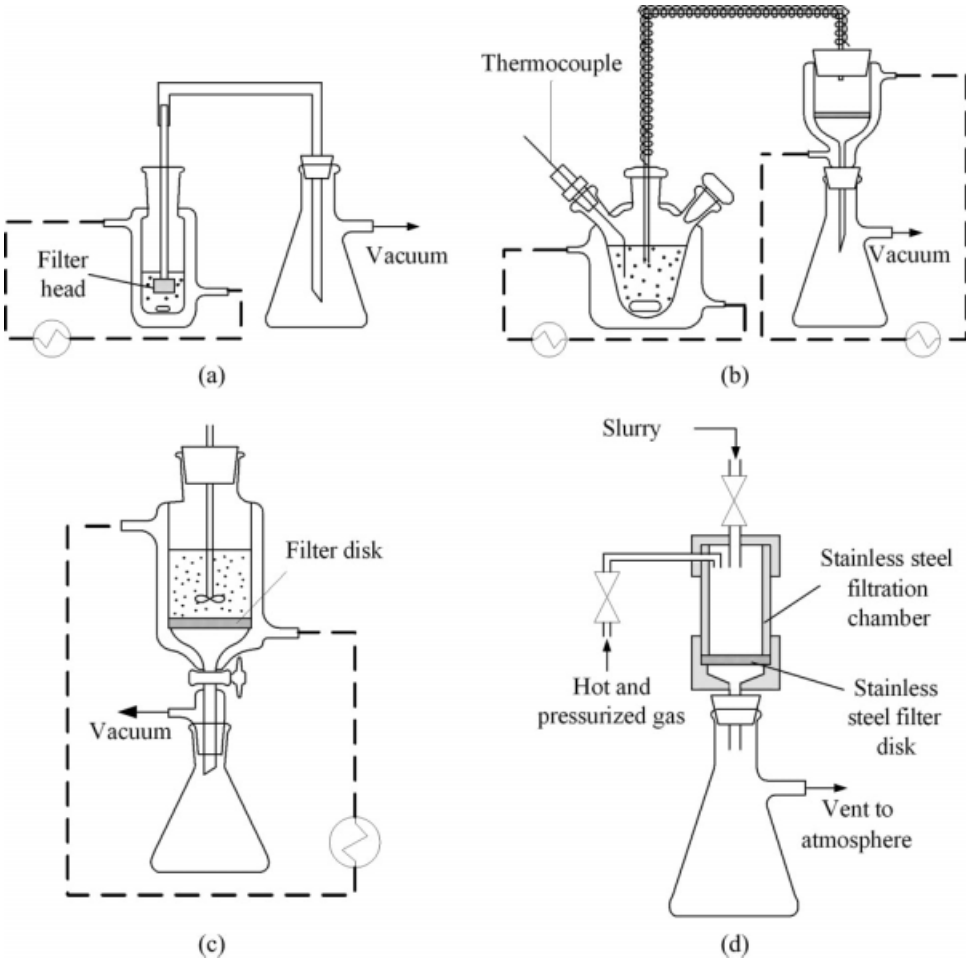

Figure 4. Basic design of bench-scale experimental setups for crystallization and solids recovery.

(a) A crystallizer with a filter head for solids recovery. (b) A separate filter for crystallization at a moderate temperature. (c) For extreme crystallization temperatures, a crystallizer/filter is used. (d) For slurry requiring high-pressure filtration, a stainless steel chamber is used.

product can be used as the wash liquid. However, the experimentalist usually needs a lot of practice to handle a saturated wash liquid properly in order not to inadvertently precipitate out the solute. Most impurities present in crystals are in ppm level. Suitable analytical procedure and related sample preparation techniques should be developed in advance, with emphasis on the sensitivity and detection limits of both product and impurities.

Case study—Ascorbic acid process

The effect of cooling rate, crystallization yield, and solvent content on the inclusion level were studied in the ascorbic acid example.

Materials and Experimental Setup. In the absence of an actual plant reactor effluent sample, a representative crystallizer feed was prepared by mixing pure chemicals, including ascorbic acid (>99%; Sigma-Aldrich), oxalic acid (99.5%; BDH), 2-furaldehye (99%; Sigma-Aldrich), ethanol (absolute >99.9%; Merck), and water. All runs were seeded using fine ascorbic acid particles obtained by recrystallization of the commercial ascorbic acid using 50 wt % ethanol in water as the solvent, followed by filtration, drying, and sieving to obtain particles in the size range of 20–45 μm. The seed particles were suspended in a saturated solution of ascorbic acid in 50 wt % ethanol in water before usage. The main purpose of this seed preparation procedure is to avoid milling, which may produce crystals that are unable to grow because of mechanical damages on their surfaces.

The crystallization experiments were carried out using the setup shown in Figure 5. The 125-ml jacketed glass crystallizer was connected to an oil circulating bath (Ministat 125, Huber) with an operating temperature range of −25°C to

Table 3. Criteria for Selection of Wash Liquid

• It is one of the components in the existing process.
• It does not adversely affect the crystal product quality such as particle size, morphology, and color.
• The product is not soluble in the wash liquid.
• It does not cause precipitation of impurities during washing.
• It can be easily removed by drying the product crystals.
• It can be easily recovered for reuse.
• It does not cause phase split with other solvents in the existing process.

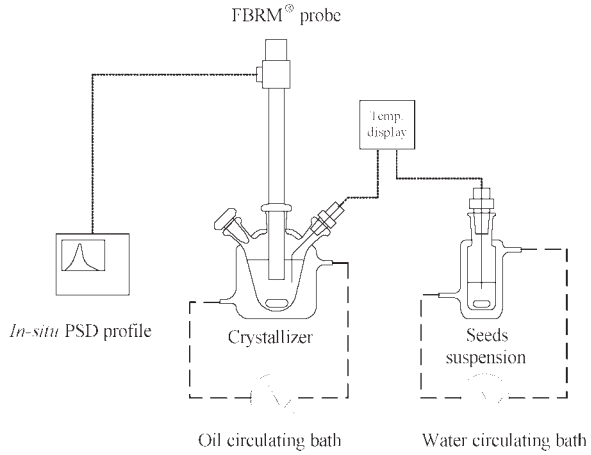

Figure 5. The experimental setup for the crystallization experiments.

150°C. A separate jacketed glass vessel containing seed suspension was kept at the dissolution temperature of the crystallization mixture by a water circulating bath. The temperatures inside both vessels were monitored using thermocouples. Mixing was provided by magnetic stirrers placed underneath the vessels. The crystallizer was equipped with a Lasentec® FBRM® (Focused Beam Reflectance Measurement) probe (D600L, Mettler Toledo) for in-situ monitoring of crystal size distribution.

Experimental Procedure. Altogether 16 runs of crystallization experiments were performed with different final crystallizer temperatures, cooling rates, and solvent concentrations. To investigate the effect of crystallization yield, several runs (Runs 1–5) were conducted with the same initial composition and temperature, but with different final crystallization temperatures. Runs 6–10 were conducted with different cooling rates. A series of runs (Runs 11–16) with a different solute to solvent ratio were also carried out, with a similar crystallization yield achieved by keeping the same temperature difference between the crystallizer feed and outlet. The crystallization conditions are summarized in Table 4.

In each run, chemicals of known compositions were weighed and mixed in the crystallizer with a constant stirring rate of 600 rpm. The mixture was heated at a rate of 0.5°C min^{-1} until all solids dissolved, at which point the dissolution temperature was recorded. The solution was then cooled to 2°C below the dissolution temperature, and 2 ml of seed suspension (10 wt % solid content) was added using a digital pipette. The seed amount was determined according to the critical seed loading ratio from the seed chart developed by Norihito et al.[22] The particle count of the seeds was monitored using the FBRM® probe. The mixture was then cooled at the desired cooling rate to the final crystallization temperature and kept overnight under constant stirring to achieve equilibrium.

At the end of the crystallization experiment, the solids were filtered out and washed thoroughly to remove surface impurities before being analyzed. As the slurry was at nearly room temperature and the volume of slurry was about 100 ml, the basic design for solid recovery in Figure 4b was used for solids recovery. Based on the selection criteria in Table 3, a saturated solution of ascorbic acid in ethanol at the crystallization temperature was chosen as the wash liquid. Approximately 1.5 ml of this solution was used to wash 1 g of crystals. For a 16 g filter cake, 24 ml wash liquid was used at one time with mild stirring using a spatula. The cake was washed four times to ensure that the surface impurities were completely removed.

After washing, strong suction was applied to remove most of the residual liquid remaining in the cake, followed by drying in a vacuum oven at room temperature overnight. Finally, the solid composition was analyzed by HPLC (Agilent 1100) using the Prevail Organic Acid column (Alltech, 5 μm) and 10 mM NaH_2PO_4 buffer solution (pH = 2.5) as the mobile phase. Each solid sample was dissolved in double deionized water to make a 1 wt % solution. This relatively high concentration was necessary to ensure detection of the ppm amount of impurity in the sample. The sample solution was passed through a 0.2 μm syringe filter before being injected to the HPLC.

Results. Figure 6a shows the inclusion impurity concentration of oxalic acid and 2-furaldehyde as a function of the

Table 4. Experimental Conditions for the Cooling Crystallization of Ascorbic Acid

Runs	Solvent, wt % (EtOH:H_2O = 50:50)	Solute, wt % (AsA:OxA:2-Fur = 27:4:4)	T_{dis} (°C)	T_{cry} (°C)	ΔT (°C)	Cooling rate (°C min^{-1})
1	65	35	48.3	33.3	15	0.5
2	65	35	48.3	28.3	20	0.5
3	65	35	48.3	23.3	25	0.5
4	65	35	48.3	18.3	30	0.5
5	65	35	48.3	8.3	40	0.5
6	65	35	48.3	28.3	20	0.05
7	65	35	48.3	28.3	20	0.1
8	65	35	48.3	28.3	20	1
9	65	35	48.3	28.3	20	2
10	65	35	48.3	28.3	20	3
11	75	25	30.2	10.2	20	0.05
12	75	25	30.2	10.2	20	0.1
13	75	25	30.2	10.2	20	0.5
14	75	25	30.2	10.2	20	1
15	75	25	30.2	10.2	20	2
16	75	25	30.2	10.2	20	3

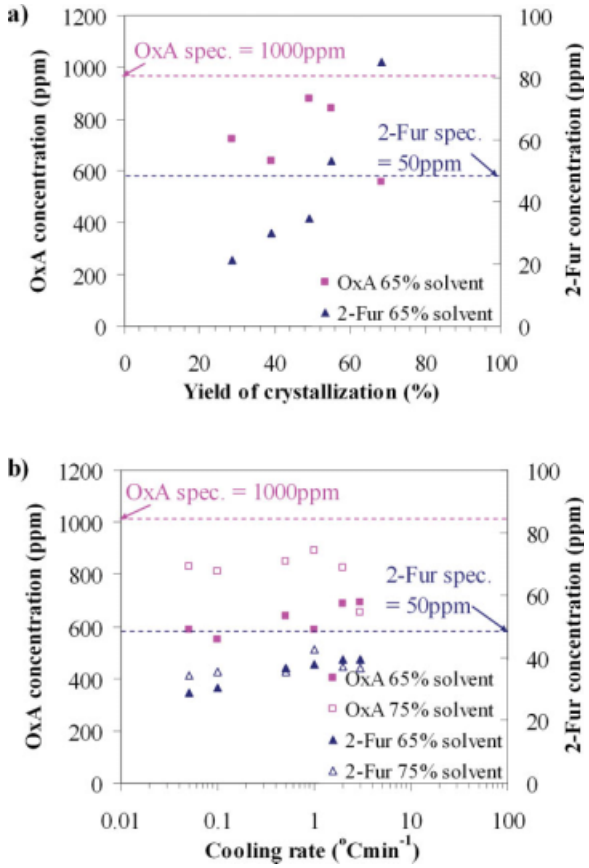

Figure 6. Inclusion impurity concentration of oxalic acid and 2-furaldehyde as a function of operating conditions.

(a) Crystallization yield and (b) cooling rate. [Color figure can be viewed in the online issue, which is available at www.interscience.wiley.com.]

crystallization yield for Runs 1–5, which were carried out at a constant cooling rate of 0.5°C min^{-1} and a feed composition of 35 wt % solute (i.e., 65 wt % solvent). A higher yield was achieved by lowering the final crystallizer temperature so that more ascorbic acid crystallized out of the solution. The concentration of 2-furaldehyde clearly increased as the crystallization yield increased, whereas the concentration of oxalic acid was bounded between 500 and 900 ppm without an obvious trend.

The effect of cooling rate is depicted in Figure 6b. Six runs (Runs 6–10 together with Run 2) were performed with the same feed composition (65 wt % solvent) and a temperature drop of 20°C (from a feed temperature of 48.3°C to a final crystallization temperature of 28.3°C). The inclusion concentrations of both oxalic acid and 2-furaldehyde showed a slightly increasing trend to cooling rate.

Six other runs (Runs 11–16) were carried out with a different feed composition (75 wt % solvent) but the same temperature drop of 20°C. Although the total solute concentration was lower, the ratio of AsA:OxA:2-Fur in the feed remained the same at 27:4:4. The feed temperature was adjusted to 30.2°C to achieve saturation of AsA. Because of the linear relationship between solubility and temperature over 10–60°C temperature range, the AsA yield of 40% is the same in both cases. The results indicate that crystals from the runs with 75% solvent contained higher concentrations of impurities, especially oxalic acid, compared with those obtained from runs with 65% solvent (Figure 6b).

Figure 7 shows the in-situ particle counts for two size ranges for Runs 2 and 6–10, based on the chord length distribution recorded by the FBRM® probe. The vertical dotted lines demarcate the end of the cooling period for each run, beyond which the slurry was kept at a constant temperature. Particles with a chord length between 1–46 μm and 46–1000 μm are referred to as "fine particles" and "large particles," respectively. Note that the cutoff size between the two size ranges has been arbitrarily chosen such that the seed particles completely fall within the fine particles range.

It can be seen that similar trends can be observed for all runs. Except for a short period at the beginning, the count of fine particles monotonically increased, whereas the count of large particles initially increased, reaching a maximum, and then decreased towards a plateau. The initial slope of the large particles curve was steeper with increasing cooling rate, suggesting faster growth at higher cooling rate as expected. However, at lower cooling rates, the peak of the large particles curve occurred during the cooling period, whereas at higher cooling rates this peak occurred during the equilibration period. This is a clear indication that ascorbic acid crystals grew relatively slowly, so that when the cooling rate was higher than 0.1°C min^{-1} (Figures 7c–f) the crystallization process was far from completion by the time the cooling stopped. Also, a relatively high supersaturation was generated with increasing cooling rate. The decrease in the number of large particles after the maximum was believed to be due to attrition caused by the magnetic stirrer. Along the same line of reasoning, the increase in the number of small particles was partly due to attrition and partly due to nucleation. The latter was a result of the residual supersaturation and the nucleation induced by the magnetic stirrer.

Based on the results shown in Figures 6 and 7, it can be concluded that reducing the cooling rate, and thus the crystal growth rate, could be the way to minimize 2-Fur and oxalic acid contents in the final product. The concentration of 2-Fur could also be controlled by manipulating the yield of crystallization.

Filtration, Washing, and Deliquoring Experiments

The reduction of surface impurities is quantified in the washing and deliquoring performance studies. In practice, washing and deliquoring are inseparable from filtration, as they often occur consecutively in a single equipment unit such as a rotary vacuum filter, a belt filter, or a centrifuge. Models for the filtration, washing, and deliquoring steps can be used to provide scale-up predictions based on the results of small-scale experiments. The values of model parameters, such as cake permeability, filter medium resistance, and diffusivity, which are difficult to predict, will be determined experimentally. The details are explained later.

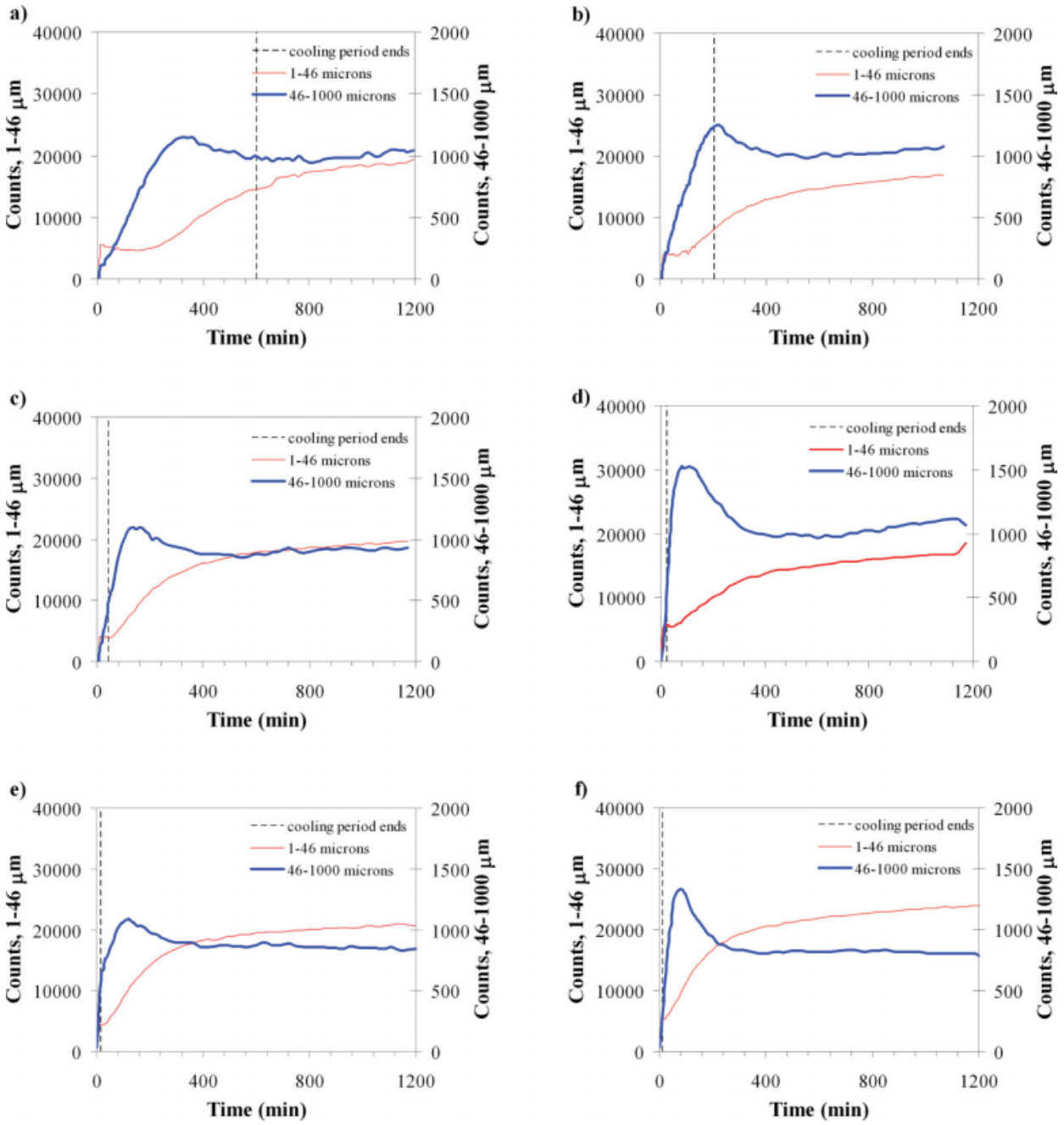

Figure 7. The number of fine particles (1–46 μm) and large particles (46–1000 μm) as a function of time at different cooling rates.

(a) Run 6 at 0.05°C min^{-1}, (b) Run 7 at 0.1°C min^{-1}, (c) Run 2 at 0.5°C min^{-1}, (d) Run 8 at 1°C min^{-1}, (e) Run 9 at 2°C min^{-1}, and (f) Run 10 at 3°C min^{-1}. [Color figure can be viewed in the online issue, which is available at www.interscience.wiley.com.]

Filtration, washing, and deliquoring models

The basic model for filtration at constant pressure is

$$\frac{t}{V} = \frac{\mu\alpha c}{2A^2\Delta p}V + \frac{\mu R_m}{A\Delta p}. \quad (1)$$

here V is the total filtrate volume collected at time t, Δp is the pressure drop, μ is the filtrate viscosity, α is the specific cake resistance, c is the mass of solids deposited in the filter per unit volume of filtrate, A is the filtration area, and R_m is the filter medium resistance. As is common in practice, α and R_m are calculated from the slope and intercept, respectively, of the plot of t/V against V.

By solving Eq. 1, in terms of total filtrate volume, design equations for specific types of equipment can be derived. For example, for a continuous belt filter, the filtrate flow rate q_F can be expressed as

$$q_F = \frac{vw}{\alpha c}\left(-R_m + \sqrt{R_m^2 + \frac{2\alpha c \Delta p L_F}{\mu v}}\right) \quad (2)$$

where v is the linear speed of the moving belt, w is the belt width, and L_F is the length of the belt section dedicated to filtration. The same equation can be used for a continuous rotary drum filter by substituting

$$v = \omega r \quad (3)$$

$$L_F = \theta_F r \quad (4)$$

where ω is the angular speed of the drum, r is the drum radius, and θ_F is the angle corresponding to the drum section dedicated to filtration. Design equations for a horizontal basket centrifuge, which take into account the dependence of Δp on the dimensions and rotational speed of the equipment, have been developed by Chan et al.[7] Once the cake and filter medium resistances have been obtained from small-scale experiments, these design equations can be used to predict the performance of the large-scale equipment.

Models for displacement washing, which is achieved by spraying wash liquid on top of the wet cake after filtration to displace the impurity-containing residual liquid from the pores of cake, have been developed by Wakeman and Tarleton.[6] When the residual liquid content during washing is constant (that is, when the wash liquid flow rate equals the filtrate flow rate leaving the cake), the concentration of an impurity in the wash liquid effluent is related to the amount of wash liquid via the expression

$$\Phi = \Phi(W, D_n) \quad (5)$$

where

$$\Phi = \frac{\phi - \phi_f}{\phi_0 - \phi_f} \quad (6)$$

$$W = \frac{\rho_L q_W t_W}{m_s X_0} \quad (7)$$

$$D_n = \frac{ux}{\varepsilon D_L} \quad (8)$$

In Eq. 6, Φ is the dimensionless wash liquid concentration, ϕ, ϕ_0, and ϕ_f are the impurity concentrations in the wash liquid effluent, residual liquid before washing, and wash liquid feed, respectively. The wash ratio W is defined in Eq. 7, where ρ_L and q_W are the density and flow rate of the wash liquid, respectively, t_W is the washing time, m_S is the mass of solids, and X_0 is the residual liquid content or wetness of the cake (i.e., the weight ratio of liquid to solids). Equation 8 defines the dimensionless dispersion number D_n, which depends on the linear velocity of filtrate u and the axial diffusivity D_L as well as on cake thickness x and porosity ε. Although curves of Φ vs. W for various values of D_n are available in the literature,[6] estimating the value of D_n is difficult. A practical approach is to perform washing experiments to obtain an empirical expression of Φ vs. W for the particular cake being washed. Assuming an even cake thickness and uniform wash liquid distribution over the cake in the bench-scale unit as well as in the large-scale equipment, the results can be used for scale up and design. For example, in a continuous belt filter, m_S/t_W in Eq. 7 can be replaced by the solids flow rate, and the impurity concentration after washing with a given wash liquid flow rate can be calculated. Furthermore, to keep the wash liquid flow rate the same as the filtrate flow rate, the length of the belt section over which the wash liquid L_W is distributed can be determined by calculating the required washing time from Eq. 1, replacing t, V, and A with t_W, $q_W \cdot t_W$, and $W \cdot v \cdot t_W$, respectively.

Deliquoring can occur as a result of two mechanisms: compaction, in which the contraction of a wet cake squeezes out a portion of the residual liquid; and desaturation, in which the residual liquid is removed by sucking or blowing gas through the cake. Compaction can be described by an empirical correlation between cake porosity and pressure difference such as

$$\varepsilon = \varepsilon_0 (\Delta p)^n, \quad (9)$$

as the reduction in residual liquid content can be attributed to the decreasing porosity as a result of compaction. A fundamental model for desaturation taking into account the two-phase flow of gas and liquid through a porous medium is available.[23] It can be solved to obtain easier-to-use correlations—the parameters of which include system-related properties, such as cake porosity, particle size, and solid–liquid interfacial tension—that allow the calculation of residual liquid content as a function of deliquoring time. In practice, however, we suggest that the curve of residual content vs. time at different levels of Δp be obtained experimentally, which is then used to determine the required deliquoring time to achieve the final wetness target at a given Δp. Scale up predictions can be made using experimental results obtained using a similar cake and at the same Δp as expected in the actual equipment.

Generic experimental design

The model parameters are highly system-dependent, care should be taken to perform the bench-scale experiments using materials that are practically identical to the actual materials to be handled in the large-scale process. In particular, the particle size distribution of the solids, which strongly affects the cake porosity and permeability, needs to be as similar as possible. If feasible, plant slurry should be used in this study and the same filter cake should be used throughout the consecutive filtration, washing, and deliquoring experiments. Table 5 summarizes the guidelines for designing filtration–washing–deliquoring experimental setup and procedure.

Such a design is shown in Figure 8. Slurry, mother liquor obtained by filtering out the crystals from the slurry, and wash liquid are stored in separate containers, and their temperatures can be maintained by external oil circulation systems. Filtration, washing, and deliquoring take place in a jacketed filter funnel that is connected to the temperature bath. The conical flask under vacuum is placed underneath the funnel to collect the filtrate. A measuring cylinder inside the flask is used to measure the filtrate volume. The jacketed

Table 5. Guidelines for Performing Filtration–Washing–Deliquoring Experiments

Slurry preparation
• If possible, use crystals from the pilot plant or the industrial plant so that realistic filter cake properties could be obtained.
• If plant samples are not available, the slurry should be made up with crystals of similar particle size distribution.
• Avoid large temperature change when transferring slurry from slurry vessel to filter.
Filtration experiments
• The setup should allow using the same filter used throughout the consecutive filtration–washing–deliquoring experiments.
• The pressure difference could be provided by vacuum, high pressure air, or nitrogen.
Washing experiments
• Wash liquid and make-up mother liquor should be kept at the washing temperature.
• A spray could be used to deliver the wash liquid evenly on the cake.
• Cake thickness should be measured before and after washing.
• To maintain constant wetness, the flow rate of wash liquid should be kept to be the same as the filtrate flow rate.
• The tubing that delivers the wash liquid to the filter cake should be well-insulated to avoid heat loss.
Deliquoring experiments
• A stainless steel filter could be used for high-pressure operations.

vessel for storing the wash liquid is connected to the top of the filter funnel by silicone tubing wrapped with fiber glass to avoid heat loss. A peristaltic pump transfers the wash liquid at a constant rate to the filter cake. To avoid accumulation of wash liquid on the filter cake, the wash liquid flow rate is maintained to be the same as the filtrate flow rate for the specified pressure difference. During washing experiments, wash liquid effluent is collected from time to time such that its composition at different wash ratios could be measured. Deliquoring is achieved by shutting off the peristaltic pump. For high-pressure experiments, as mentioned earlier, the glass filter in Figure 8 could be replaced by a stainless steel filter shown in Figure 4d. Pressurized and temperature controlled air is passed into the filter to provide the driving force for filtration, washing, and deliquoring. It is possible to use nitrogen gas instead of air for air-sensitive systems.

Case study—Ascorbic acid process

Materials and Experimental Setup. In the absence of the actual slurry from a large-scale crystallizer, fresh ascorbic acid crystals were mixed with a solution having the same composition as the expected mother liquor from crystallization. The make-up slurry was prepared using 16 g of fresh ascorbic acid crystals and 84 g of mother liquor containing 18.55 wt % AsA, 4.35 wt % OxA, 4.35 wt % 2-Fur, and 72.75 wt % solvent (ethanol/water 50/50), which gives a magma density of 0.16 (kg of solids/kg of total slurry). All chemicals were from the same sources as those used for the inclusion experiments. As the slurry was near room temperature and crystal growth of the ascorbic acid was slow in response to temperature drop, the original design for filtration–washing–deliquoring experiments in Figure 8 was used.

Experimental Procedure. At the beginning of the filtration experiment, the jacketed filter funnel was preheated to the crystallization temperature, which was 28°C for all the runs in this study. The slurry was then poured into the filter funnel and the vacuum pump was turned on, keeping the pressure difference constant at 10 kPa. The entire filtration process was videotaped so that the volume of filtrate collected in the measuring cylinder over time was recorded. In this case, the final filtrate flow rate of 0.1 ml s^{-1} was measured.

The cake from the filtration experiment was used in the subsequent washing experiment. As the cake was almost dry at the end of the filtration experiment due to prolonged application of vacuum, fresh mother liquor had to be added to obtain a filter cake with the desirable cake wetness. To imitate the condition at the end of an actual filtration process, 60 ml of mother liquor was poured onto the filter cake and the excess was removed under a vacuum of $\Delta p = 10$ kPa. By monitoring the amount of mother liquor, the cake wetness was determined to be 0.18. As soon as the liquid level reached the cake surface, both the peristaltic pump and the vacuum pump were started at the same time. The flowrate of wash liquid, which has the same density as that of mother liquor, was maintained at 0.1 ml s^{-1}. This value was the same as the final filtration flowrate recorded in the filtration step. Seven fractions of the wash liquid effluent were collected in seven 100-ml conical flasks at 6, 11, 19, 23, 27, 31, and 38 s after the washing started, corresponding to wash ratios of 0.2, 0.4, 0.7, 0.8, 1.0, 1.1, and 1.4, respectively. These fractions were analyzed using HPLC. Only washing performance with respect to oxalic acid was investigated, as 2-furaldehyde because of its volatility was expected to be removed during drying.

The deliquoring experiment immediately followed the washing experiment. The same wet cake in the filter funnel was used. In the first run, the liquid in the wet filter cake was sucked out under the same vacuum level as in the washing experiments ($\Delta p = 10$ kPa). Similar to the filtration experiment, the entire process was videotaped and the volume of liquid collected in the measuring cylinder was recorded from time to time. The residual liquid content in the cake was calculated from material balance. To investigate the effect of vacuum level on deliquoring performance, the procedure was repeated to perform two more runs with

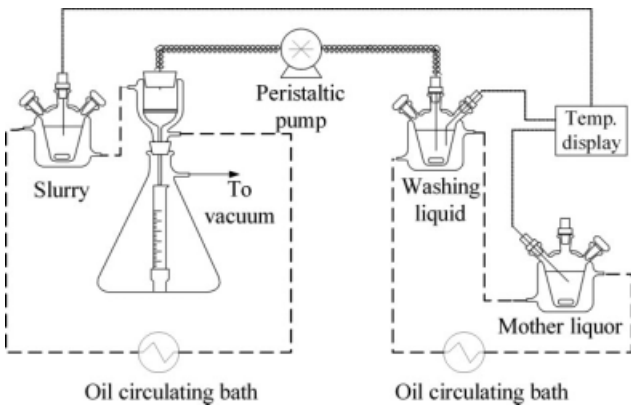

Figure 8. A bench-scale experimental setup for the filtration, washing, and deliquoring experiments.

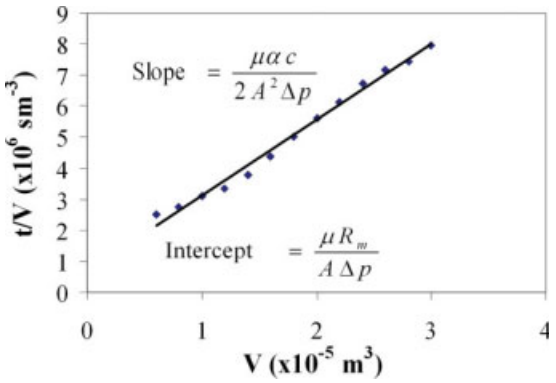

Figure 9. A plot for determining the specific cake resistance and the medium resistance.

[Color figure can be viewed in the online issue, which is available at www.interscience.wiley.com.]

Δp of 6.7 and 13.3 kPa. The filter cake was made up to the same wetness at 0.18 by carefully adding the corresponding amount of wash liquid into it before a new deliquoring experiment began.

Results. Figure 9 shows a plot of t/V vs. V obtained from the results of the filtration experiment. The filtrate viscosity was measured to be 0.0204 Pa s, the filter area was 0.0013 m^2, and c was 203 kg m^{-3}. From the slope and intercept, $\alpha = 1.85 \times 10^9$ m kg^{-1} and $R_m = 4.28 \times 10^8$ m^{-1}. A final filtrate flow rate of 0.1 ml s^{-1} was measured. The washing performance in terms of dimensionless wash liquid effluent concentration of OxA vs. wash ratio is plotted in Figure 10. The overall trend of this curve can be captured using a two-parameter model

$$\Phi = \frac{1}{a + (1-a)\exp(bW)} \tag{10}$$

Fitting the experimental data to the model, the parameters a and b were determined to be -1.58×10^{-3} and 1.21, respectively. Note that this is not only the expression that can be used to fit the data, but also the most suitable model to represent the data may differ from system to system. The

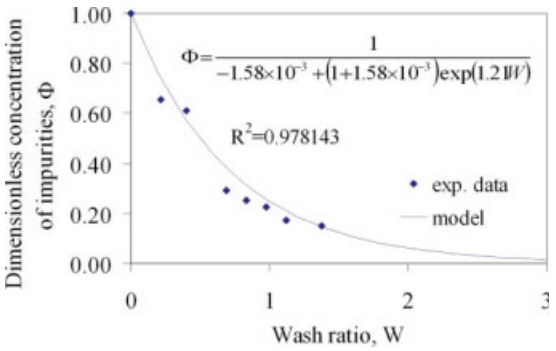

Figure 10. Dependence of the dimensionless concentration of oxalic acid on wash ratio.

[Color figure can be viewed in the online issue, which is available at www.interscience.wiley.com.]

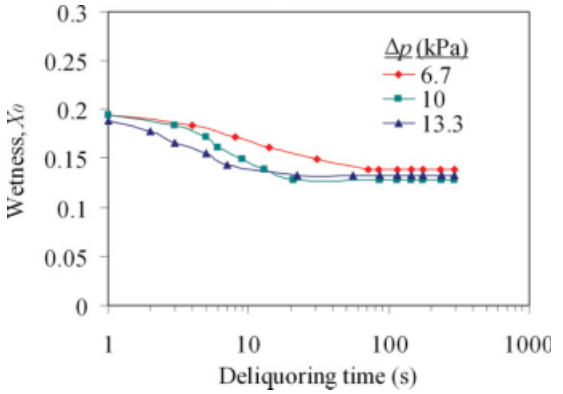

Figure 11. Dependence of wetness of filter cake on deliquoring time at difference ΔP values.

[Color figure can be viewed in the online issue, which is available at www.interscience.wiley.com.]

results of the deliquoring experiments are shown in Figure 11. Clearly, the required deliquoring time to achieve a given cake wetness depends on Δp. In general, a higher Δp would lead to a lower wetness at the same deliquoring time. The flat portion of the curves at long deliquoring time represents the irreducible saturation.

Conceptual Design

The crystallization and downstream processes can be synthesized using the systematic procedure proposed by Chang and Ng.[8] Rules and heuristics are provided for determining the required unit operations, the destinations of the reaction solvent, mother liquor, wash liquid, recrystallization solvent, and drowning-out solvent, if any. One of the key considerations is whether recrystallization is needed. If inclusion impurities can be kept below the product specification by modifying the crystallizer design or manipulating the operating conditions, no recrystallization is needed. Washing and deliquoring alone can be used to provide an on-spec final product. When the amount of inclusion impurities is above product specification, recrystallization is essential. For each conceptual design, material balance of the overall process is performed to identify potential trade-offs. For example, it may be possible to meet the desired purity specifications using two crystallization stages with a relatively high per-pass yield in each step or using just one stage but with a much lower per-pass yield as well as better washing and deliquoring.

Case study—Ascorbic acid process

Scenario I: Single Crystallization Stage. Based on the results of inclusion study shown in Figures 6a, b, it is possible to keep 2-furaldehyde concentration below the specified maximum of 50 ppm as long as the yield of crystallization does not exceed 55%. As the oxalic acid concentration is also below the maximum level of 1000 ppm for all tested crystallization conditions, it is possible to meet the product specifications without a recrystallization step.

The process flow sheet for this scenario is shown in Figure 12. The reactant D-glucose and the reaction solvent

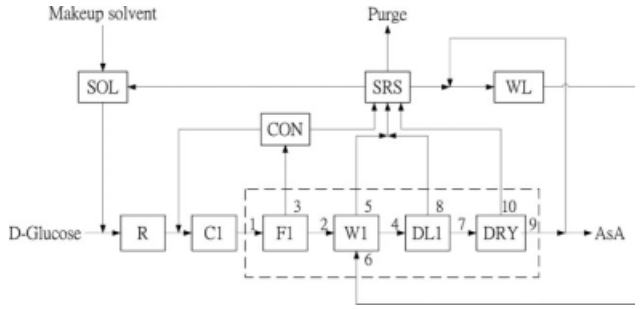

Figure 12. The Scenario I flow sheet for the ascorbic acid crystallization and downstream process.

(50 wt % ethanol in water) are fed to the reactor (R) to produce ascorbic acid. The conversion of D-glucose is close to 100%. For this case study, we assume D-glucose reacts completely in one pass and thus recycle of the reactant is not considered. The reaction effluent is fed to the crystallizer to recover pure AsA. The slurry from the crystallizer (C1) goes through the filtration (F1), washing (W1), and deliquoring (DL1) steps. The filtrate is sent to the concentrator (CON) and its concentrate is recycled to the crystallizer. The solvent from the concentrator is sent to the solvent recovery system (SRS). A saturated solution of ascorbic acid in the solvent (ethanol) is used as wash liquid. This wash liquid is prepared by dissolving part of product AsA and delivered to the washing unit from the wash liquid (WL) tank. After washing, the filter cake further goes through deliquoring and drying (DRY) to give the final product. The effluent streams from washing, deliquoring, and drying are sent to the solvent recovery system. The details of treating the azeotropic ethanol–water solution will not be discussed in this article. From the solvent recovery system, one stream is returned to the solvent tank (SOL) and another one that contains ethanol is sent to the wash liquid tank. Impurities are purged to avoid accumulation in the system.

Assuming that the crystallizer is operated under the same conditions as Run 2 in the inclusion study, product crystals with 650 ppm OxA and 30 ppm 2-Fur as impurities are produced. To meet the product specifications, the maximum amount of OxA and 2-Fur as surface impurities must not exceed 350 ppm and 20 ppm, respectively. As 2-Fur is volatile and removable by the drying process, only OxA is considered in the subsequent analysis.

For simplicity, only a selected section of the flow sheet in Figure 12 (Streams 1–10) is considered for material balance (Table 6). The slurry from the crystallizer to the filter (Stream 1) contains 329.9 kg h^{-1} liquid and 40 kg h^{-1} solids. From the results of the filtration experiments, if a vacuum level of 10 kPa is chosen, the wetness of the filter cake is 0.184 and the liquid flow rate in Stream 2 is 7.4 kg h^{-1}. With the assumption of constant wetness throughout washing, the liquid content in Stream 4 also equals 7.4 kg h^{-1}. The amount of wash liquid is 7.4 $\times$ W kg h^{-1}, where W is the wash ratio, which is defined as the mass ratio of wash liquid to mother liquor content in the filter cake (Eq. 7). Applying the same vacuum level of 10 kPa for deliquoring, the final wetness after deliquoring is 0.127, as shown in Figure 11, and thus the liquid flow rate of 5.1 kg h^{-1} for Stream 7 is calculated. To achieve a final impurity content of 1000 ppm in the AsA product, assuming that all solvent and 2-Fur is removed during drying, the required $y_{OxA,7}$ is 2763 ppm. As $y_{OxA,7} = y_{OxA,8} = y_{OxA,4}$, $y_{OxA,4}$ can be calculated as a function of W using the empirical washing model (Eq. 10). As a result, to meet the target of $y_{OxA,7} = 2763$ ppm, the minimum value of W is 2.00.

Different inclusion levels may result from changes in crystallization conditions in subsequent design stages or in the actual plant, and different purity specifications may come from changes in marketing strategies or special requirements from the customer. With the models and correlations representing the inclusion and filtration–washing–deliquoring performances in place, it is straightforward to determine the required wash ratio for the different cases. Figure 13 shows the wash ratio required to meet a product purity target (1000, 750, and 500 ppm) for various values of OxA inclusion level. In general, the required wash ratio increases sharply as the impurity inclusion level approaches the target impurity level in the final product. For instance, if the target specification is tightened to 750 ppm, and the inclusion level stays the same at 650 ppm, a wash ratio of 2.9 would be needed. On the other hand, if the inclusion level of OxA can be reduced to 500 ppm by further adjusting the operations of crystallization, a wash ratio of 2.4 is sufficient to achieve the product specifications of 750 ppm.

Scenario II: Multiple Crystallization Stages. Another possible scenario is that the inclusion impurity level in the first crystallization stage always exceeds the final product specification, regardless of the crystallization conditions. For example, the experimental data indicate that if the specifications of OxA and 2-Fur were 50 ppm and 5 ppm, respectively, varying the crystallization conditions within the acceptable range will not result in an inclusion level below the target. Therefore, the only way to meet the specifications is to dissolve the crystals in a fresh solvent, and recrystallize the product from the solution. As the impurity concentration in this solution will be lower than in the previous crystallization stage, a lower inclusion level in the solids can be expected.

Figure 14 shows the process flow sheet for this scenario, in the case of three crystallization stages. After the first

Table 6. The Stream Table for the Filtration–Washing–Deliquoring Section of the Ascorbic Acid Plant in Figure 12

Streams	1	2	3	4	5	6	7	8	9	10
L_i (kg h^{-1})	329.9	7.4	322.6	7.4	14.7	14.7	5.1	2.3	–	5.1
$y_{OxA,i}$ (ppm)	44,768	44,768	44,768	2763	13,831	0	2763	2763	–	0
$y_{2\text{-}Fur,i}$ (ppm)	44,843	44,843	44,843	2768	13,854	0	2768	2768	–	2779
S_i (kg h^{-1})	40	40	0	40	0	0	40	0	40	0
$x_{OxA,i}$ (ppm)	650	650	–	650	–	–	650	–	1000	–
$x_{2\text{-}Fur,i}$ (ppm)	30	30	–	30	–	–	30	–	30	–

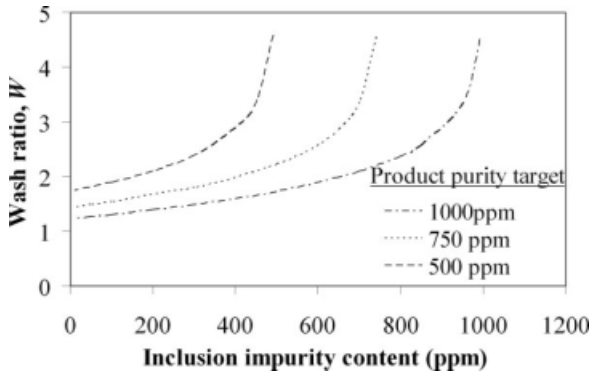

Figure 13. The wash ratio required to meet product purity target for a specified inclusion impurity content.

filtration–washing–deliquoring train (F1-W1-DL1), the solids (Stream 8) are sent to the second crystallization stage, which consists of dissolver DS1, crystallizer C2, and filtration–washing–deliquoring train F2-W2-DL2. Stream 18 is then sent to a dissolver DS2 and then the third crystallization stage (C3-F3-W3-DL3) before finally reaching the dryer (DRY). The recycling pattern can be extended when more crystallization stages are required according to the rules for process synthesis.[8] Outlet streams from a later crystallization stage (with lower impurity content) are recycled to an earlier crystallization stage (where the impurity content is higher) as either dissolving solvent or wash liquid. For example, the wash liquid effluent from W2 (Stream 16) and liquid effluent from DL2 (Stream 19) are used as the wash liquid for W1, as they contain considerably less impurities compared with the mother liquor from C1. Similarly, Streams 26 and 29 serve as the wash liquid for W2. Fresh or regenerated wash liquid contains the least amount of impurity is used in W3 to ensure the highest product purity. Also, the filtrate from F3 (Stream 24) can be recycled to DS1 as dissolving solvent. Fresh or regenerated solvent containing the least amount of impurity is used as dissolving solvent for DS1 and DS2.

Clearly, the required number of crystallization stages depends on the inclusion behavior and filtration–washing–deliquoring performance in each stage. Particularly important is the inclusion reduction ratio in each crystallization stage (e.g., $x_{OxA,2}/y_{OxA,1}$, $x_{OxA,12}/y_{OxA,10}$, $x_{OxA,22}/y_{OxA,20}$). Inclusion study, washing, and deliquoring experiments must be conducted for each stage.

Equipment Targeting

The experimental results, models, and correlations obtained from the washing and deliquoring performance studies are used for scale up, as long as similar cake properties can be expected in the large-scale unit. Coupled with the overall material balance model, they can be used to target the specifications of the solid–liquid separation equipment, such as a rotary vacuum filter, belt filter, or a centrifuge. In this way, the search for a suitable equipment unit can be limited to a much narrower field. For example, if it is desirable to remove more surface impurities, a centrifuge that is capable of reducing the residual liquid content to 5–7% may have to be used instead of a rotary vacuum filter that tends to offer a 20–30% content. Furthermore, design specifications for selected equipment can also be targeted. For example, the required length of a continuous belt filter, which consists of filtration, washing, and deliquoring sections, for

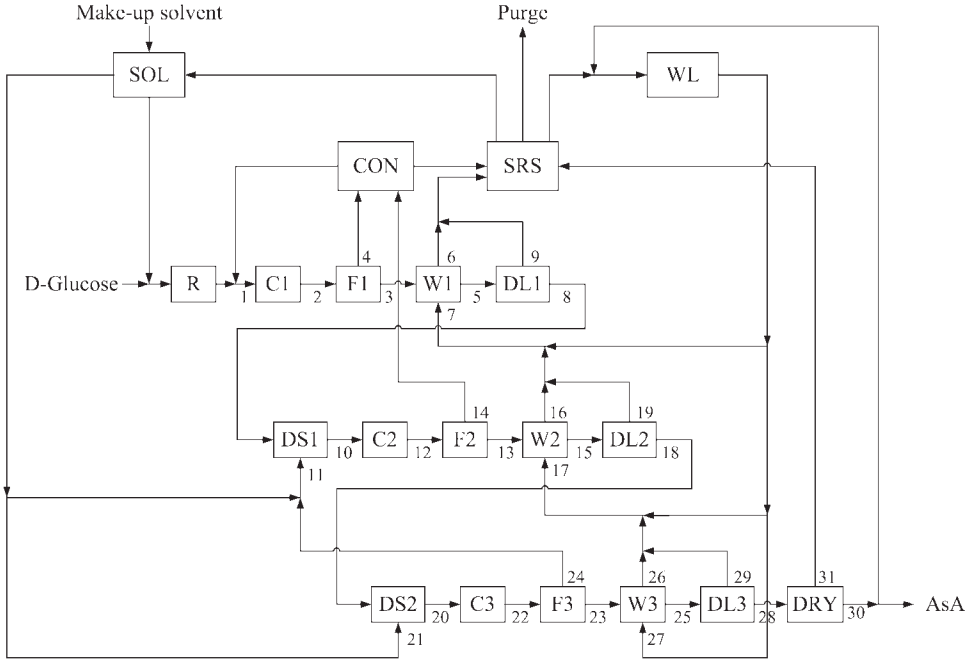

Figure 14. The Scenario II flow sheet for the ascorbic acid crystallization and downstream process with recrystallization.

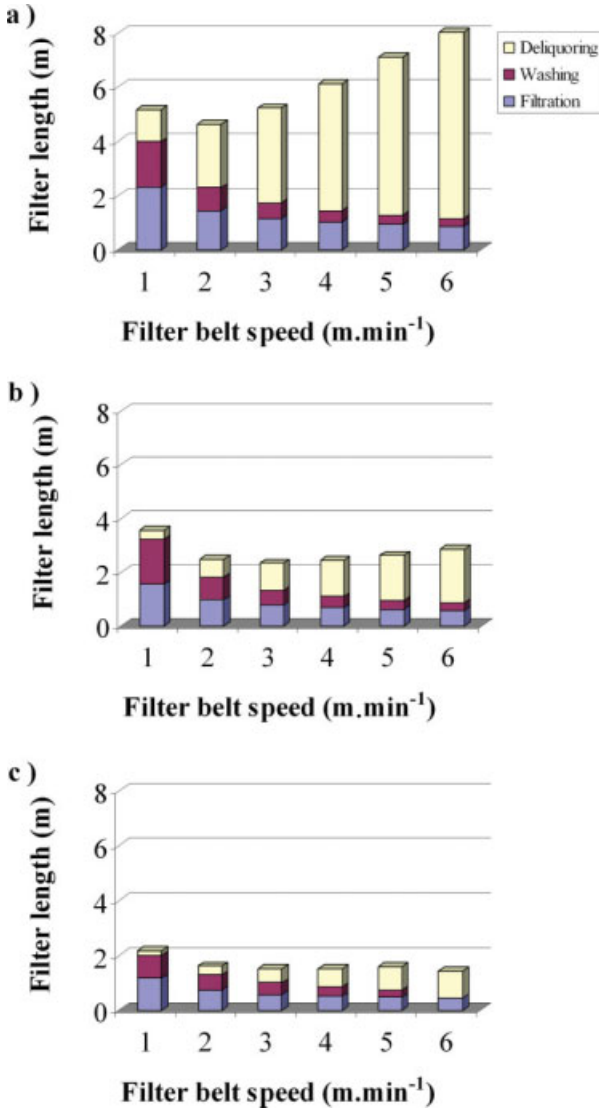

Figure 15. Variation of the filter lengths for filtration, washing, and deliquoring sections with filter belt speed for different ΔP values of (a) 6.7 kPa, (b) 10 kPa, and (c) 13.3 kPa.

[Color figure can be viewed in the online issue, which is available at www.interscience.wiley.com.]

the desired production rate can be determined for various values of filter belt speed and Δp. In selecting the appropriate speed, it is important to note that cake thickness strongly depends on the filter belt speed.

Case study—Ascorbic acid process

Figure 15 shows the calculation results for the filter lengths for filtration, washing, and deliquoring for the ascorbic acid example, with a production rate of 40 kg h^{-1} and belt width of 0.4 m. In general, a slower filter belt speed corresponds to a longer filtration time and a thicker cake to achieve the desired production rate. The washing time with the same wash ratio will also be longer as the wash liquid effluent flow rate out of the cake becomes smaller with the thicker cake. However, as deliquoring time is not a strong function of cake thickness, a shorter deliquoring section is sufficient. It can be seen in Figures 15a, b that this tradeoff leads to an optimum speed that minimizes the total filter length. Although vendors normally supply belt filters with standard dimensions and specifications, the calculated values should provide a good reference for picking the most suitable unit.

Conclusions

This research was motivated in part by the fact that most academic studies in the process systems engineering literature do not emphasize the role of experiments in process synthesis. Although it might be possible to synthesize a distillation system using correlations from a thermodynamic database, it is difficult to synthesize a complete process, which requires reaction kinetics, crystallization kinetics, filtration performance, and other process parameters that are hard to predict from theories alone. Also, as discussed previously,[10] a hierarchy of models should be used to correlate these data. Shortcut models often capture enough of the relevant physical and chemical phenomena for process synthesis[24] whereas detailed models can provide additional insights. Another motivating factor is the absence of discussions on how experiments, modeling, and synthesis should be integrated. In our experience, these efforts should proceed sequentially as well as concurrently in an iterative manner to be effective.

To systematize these tasks for process development, a number of commonsensical concepts have been articulated in this article. These include the multi-level hierarchical objective-time chart for promoting the transparency of the organization of an R&D project and the execution of its various tasks in parallel, and the workflow diagram for signifying the key iterative loops. The tasks in process development are performed using the *RAT²IO module* in an attempt to make plain the activities, resources, etc. that are involved in completing such a task. These tasks can be referred to as unit tasks to reflect their roots in unit operations in chemical engineering. Obviously, a unit task becomes a unit operation if one only focuses on the chemical engineering principles of the unit. For example, subobjective 2.3 in Figure 1, study of washing and deliquoring, involves all the management issues as well as the corresponding unit operation models.

To carry out the necessary tasks efficiently, it is crucial that the experimental setups are categorized and the appropriate level of modeling is specified. As these tasks are domain-specific, they are illustrated by the management of impurity in a crystallization process, which involves downstream processing units such as filtration, washing, and deliquoring. The heuristics and know-how that have been accumulated over a number of years are summarized for the users of this approach. The activities or tasks are purposefully scheduled in an objective-time chart (Figure 1) whereas the iterative nature of the technical tasks is captured in a workflow diagram (Figure 16). The technical activities start with SLE study to identify the crystallization region in the phase diagram to avoid cocrystallization. Inclusion experiments are carried out under a specified set of crystallization conditions. The filtration–washing–deliquoring experiments as well as data regression follow. All of this information is used in process conceptualization in which different process

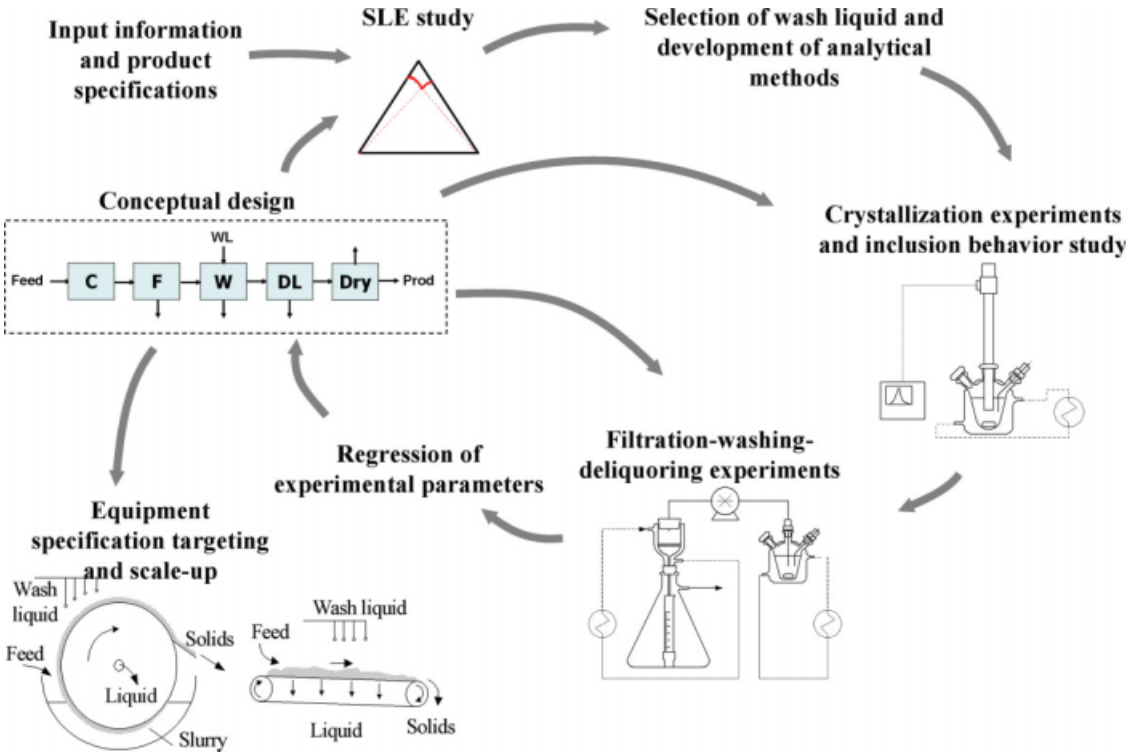

Figure 16. Workflow diagram for integrated crystallization and downstream process development.

[Color figure can be viewed in the online issue, which is available at www.interscience.wiley.com.]

alternatives are generated. Often, product specifications, flow rates in the process streams or process economics would point to an alternative that needs additional experimental investigation, be that SLE data, inclusion behavior or washing data.

Although the workflow described here closely imitates the real situation in industrial process development projects, it is not meant to offer a fixed solution to this type of problems for any given system. Rather, it highlights the key components around which an R&D organization can define its own workflow that best suits its needs, objectives, and expertise. Properly executed, significant savings in terms of the required time, effort, and money can be realized in the synthesis of crystallization downstream processes. Effort in extending this approach to other generic processes is under way.

Acknowledgment

Research support of the Research Grants Council (Grant HKUST618207) is gratefully acknowledged.

Notation

a = empirical model parameter for washing
A = filter area, m^2
b = empirical model parameter for washing
c = mass of solids per unit volume of filtrate, kg m^{-3}
D_L = axial diffusivity, m^2 s^{-1}
D_n = dimensionless dispersion number
L_F = length of filtration section, m
L_W = length of washing section, m
L_i = mass flow rate of liquid for stream i, kg h^{-1}
m_s = mass of solids, kg
n = empirical model parameter for Eq. 9.
Δp = pressure difference, Pa
q_F = volumetric flow rate of filtrate, m^3 s^{-1}
q_W = volumetric flow rate of wash liquid, m^3 s^{-1}
r = radius of rotary drum filter, m
R_m = medium resistance, m^{-1}
S_i = mass flow rate of solids for stream i, kg h^{-1}
t = time, s
t_W = washing time, s
T_{cry} = temperature of crystallization, °C
T_{diy} = temperature of dissolution, °C
ΔT = temperature difference, °C
u = filtrate flux, m s^{-1}
v = linear speed of moving filter belt, m s^{-1}
V = filtrate volume, m^3
w = filter width, m
W = wash ratio
x = cake thickness, m
X_0 = cake wetness, kg of liquid per kg of dry cake
$y_{2\text{-Fur},i}$ = 2-furaldehyde concentration in liquid phase of stream i, ppm
$y_{OxA,i}$ = oxalic acid concentration in liquid phase of stream i, ppm
$x_{2\text{-Fur},i}$ = 2-furaldehyde concentration in solid phase of stream i, ppm
$x_{OxA,i}$ = oxalic acid concentration in solid phase of stream i, ppm

Greek letters

α = specific cake resistance, m kg^{-1}
ε = porosity
ε_0 = original porosity of the filter cake
ϕ = solute concentration of wash liquid effluent, ppm
ϕ_f = solute concentration in wash liquid feed, ppm
ϕ_0 = solute concentration in residual liquid prior to washing, ppm
Φ = dimensionless wash liquid effluent concentration

μ = filtrate viscosity, Pa s
θ_F = angle corresponding to filtration section in a rotary drum filter, rad
ρ = density, kg m^{-3}
ω = angular speed of rotary drum filter, rad s^{-1}

Subscripts

S = solid
L = liquid
i = stream number

Literature Cited

1. Denbigh KG, White ET. Studies on liquid inclusions in crystals. *Chem Eng Sci*. 1966;21:739–754.
2. Kitamura M, Nakamura T. Inclusion of amino acids and the effect on growth kinetics of L-glutamic acid. *Powder Tech*. 2001;121:39–45.
3. Zhang GGZ, Grant DJW. Formation of liquid inclusions in adipic acid crystals during recrystallization from aqueous solutions. *Cryst Growth Des*. 2005;5:319–324.
4. Meadhra RÓ, Lin R. Modelling of alditol impurity incorporation into galactitol crystals. *Trans IChemE A*. 2006;84:711–720.
5. Derdour L, Févotte G, Puel F, Carvin P. Real-time evaluation of the concentration of impurities during organic solution crystallization. *Powder Tech*. 2003;129:1–7.
6. Wakeman RJ, Tarleton ES. *Filtration: Equipment Selection, Modelling and Process Simulation*, *1st ed*. Oxford, UK: Elsevier Advanced Technology, 1999.
7. Chan SH, Kiang S, Brown MA. One-dimensional centrifugation model. *AIChE J*. 2003;49:925–938.
8. Chang WC, Ng KM. Synthesis of processing system around a crystallizer. *AIChE J*. 1998;44:2240–2251.
9. Wibowo C, Chang WC, Ng KM. Design of integrated crystallization systems. *AIChE J*. 2001;47:2474–2492.
10. Ng KM, Wibowo C. Beyond process design: the emergence of a process development focus. *Korean J Chem Eng*. 2003;20:791–798.
11. Ng KM. MOPSD. A framework linking business decision-making to product and process design. *Comp Chem Eng*. 2004;29:51–56.
12. Kuellmer V. *Ascorbic acid*. In: Kirk RE, Othmer DF, editors. *Kirk-Othmer Encyclopedia of Chemical Technology (Volume 25)*. New York: Wiley, 2000:17–47.
13. Kwok KS, Chan HC, Chan CK, Ng KM. Experimental determination of solid-liquid equilibrium phase diagrams for crystallization-based process synthesis. *Ind Eng Chem Res*. 2005;44:3788–3798.
14. Day CY, Chang C, Chen CY. Phase equilibrium of ethanol + CO_2 and acetone + CO_2 at elevated pressures. *J Chem Eng Data*. 1996;41:839–843.
15. Lin C, Ng KM, Wibowo C. Producing nanoparticles using precipitation with compressed anitsolvent. *Ind Eng Chem Res*. 2007;46:3580–3589.
16. Yi Y, Hatziavramidis D, Myerson AS, Waldo M, Beylin VG. Development of a small-scale automated solution measurement apparatus. *Ind Eng Chem Res*. 2005;44:5427–5433.
17. Chan YC. Solubility Measurement Apparatus for Rapid Determination of Solid-Liquid Equilibrium Behavior, *MPhil Thesis*. Hong Kong: The Hong Kong University of Science and Technology, 2008.
18. Lin SW, Ng KM, Wibowo C. Integrative approach for polymorphic crystallization process synthesis. *Ind Eng Chem Res*. 2007;46:518–529.
19. Lam WH, Ng KM. Diastereomeric salt crystallization synthesis for chiral resolution of ibuprofen. *AIChE J*. 2007;53:429–437.
20. Lin SW, Ng KM, Wibowo C. Synthesis of crystallization processes for systems involving solid solutions. *Comp Chem Eng*. 2008;32:956–970.
21. Wibowo C, Ng KM. Visualization of high-dimensional phase diagrams of molecular and ionic mixtures. *AIChE J*. 2002;48:991–1000.
22. Norihito D, Noriaki K, Masaaki Y, Angelo C. Determination of critical seed loading ratio for the production of crystals of uni-modal size distribution in batch cooling crystallization of potassium alum. *J Chem Eng Japan*. 2002;35:670–676.
23. Wakeman RJ. The performance of filtration post-treatment processes, Part 1: The prediction and calculation of cake dewatering characteristics. *Filtrat Sep*. 1979;16:655–660.
24. Douglas JM. *Conceptual Design of Chemical Processes*. New York: McGraw-Hill, 1988.

Manuscript received Oct. 20, 2008, and revision received Jun. 15, 2009.